Differential Evolution Algorithm-Aided Time-Varying Carrier Frequency Offset Estimation for OFDM Underwater Acoustic Communication

Haijun Wang [1] , **Weihua Jiang** [2], **Qing Hu** [1,*], **Jianjun Zhang** [1] and **Yanqing Jia** [1]

1. School of Ocean Engineering and Technology, Sun Yat-sen University, Zhuhai 519000, China
2. Department of Marine Technologies, University of Haifa, Haifa 3498838, Israel
* Correspondence: huqing3@mail.sysu.edu.cn; Tel.: +86-135-8837-3692

Abstract: Orthogonal frequency division multiplexing (OFDM) is the preferred scheme for high-speed communication in the field of underwater acoustic communication. However, it is very sensitive to the carrier frequency offset (CFO). This study used a time-varying CFO estimation method aided by the differential evolution (DE) algorithm to accurately estimate the CFO of an OFDM system. This method was based on the principle that the received OFDM signal with inter-carrier interference could be considered by a Multi Carrier-code division multiple access (MC-CDMA) system on the receiver side because MC-CDMA is a technology that combines OFDM and code division multiple access (CMDA). Because it is suitable for solving problems where there are dependencies between adjacent variables, the DE algorithm was used to capture the varying CFO values on the adjacent blocks. The spreading code of the MC-CDMA was obtained based on the estimated CFO values, which were elements in the DE solutions. Then the received signal was reconstructed. The Root-Mean-Square Error between the reconstructed and actual received signals was used as the cost function, and the CFO was estimated using the DE algorithm because of its powerful parallel search capability. The simulation results showed that the proposed method had a high estimation accuracy. Compared with other intelligent optimization algorithms such as the genetic algorithm and simulated annealing mutated-genetic algorithm, the time-varying CFO estimation performance of the DE algorithm was better because of its unique ability to solve problems with dependencies between adjacent variables. Specifically, under the condition of a high signal-to-noise ratio, the improvement of estimation accuracy reaches 36.13%, and the Bit Error Rate of demodulation is thus reduced by 75%, compared with the reference algorithms. In addition, the proposed method also has good applicability to modulation methods. For phase-shift keying and quadrature amplitude modulation, in particular, the proposed method not only achieved high-precision time-varying CFO estimation values, but also reduced the demodulation deterioration caused by noise.

Keywords: orthogonal frequency division multiplexing; differential evolution algorithm; time-varying carrier frequency offset estimation; code division multiple access

1. Introduction

Orthogonal frequency division multiplexing (OFDM) was developed from multi-carrier modulation technology and has the characteristic of anti-narrowband interference [1]. The spectral efficiency of the communication process was improved by the adoption of overlapping sub-carrier modulation technology, which reduces the communication bandwidth. Because of these advantages, OFDM has become the preferred technical solution for high-rate underwater acoustic communication [2]. As its name suggests, orthogonality between sub-carriers can maximize the spectral efficiency and reduce inter-carrier interference (ICI) [3,4]. The presence of carrier frequency offset (CFO) in a communication system can destroy the orthogonality, which reduces the signal-to-noise ratio (SNR) and intensifies the ICI, significantly increasing the bit error rate (BER) of the received OFDM signal [5]. Therefore,

estimating and compensating for the CFO before demodulating and decoding the received signal is an important research objective for OFDM systems. Because of factors such as the sea surface fluctuation effect, turbulence, and internal wave motion, the transmitter and receiver terminals used in underwater communication usually have relative velocities, which leads to the Doppler effect. An approximate Doppler value is commonly estimated for each OFDM frame, and a resampling method is used for compensation after receiving the signal [6]. Because the transmitted OFDM symbol is a wideband signal, there is a residual Doppler frequency shift in the system after resampling, which can be regarded as a result of the CFO [7].

Presently, the methods used for CFO estimation can be mainly divided into two categories [8,9]: data-aided estimation [10–12] and non-data-aided estimation [13]. When the data-aided estimation is performed in the time domain, it utilizes a training sequence [10], whereas if it is performed in the frequency domain, it uses pilot symbols [11,12,14]. The non-data-aided estimation methods are also commonly referred to as blind estimation. Some auxiliary information about the received signal is used for blind channel estimation, but this does not increase the overhead of the channel resources. This information usually includes pre-set structures and characteristics such as the cyclic prefix (CP) in OFDM [15–18], responses on the null subcarrier [19–21], constant modulus [22–24], and non-Gaussianity of modulated signals [25]. In addition to the blind estimation method, Li et al. proposed that OFDM with ICI could be regarded as a multi-carrier-code division multiple access (MC-CDMA) system on the receiver side [26] because MC-CDMA is a technology that combines OFDM and code division multiple access (CMDA). Moreover, the ICI matrix in OFDM is an orthogonal matrix. An $N \times N$ ICI matrix acts as a spreading code matrix; thus N data symbols in the OFDM are spread over all N subcarriers in the MC-CDMA system [26]. The data symbols quantize the normalized CFO, obtaining M spreading code matrices as candidates. The received signal is then decoded, decided, and reconstructed using candidates. The Euclidean distance is utilized to measure the difference between the reconstructed and received signals. The result with the smallest difference value corresponds to the best-normalized CFO estimation. The scheme should be able to perfectly cancel the ICI caused by the CFO. In 2013, a joint estimation method for the CFO and channel information that embedded the channel estimation block was proposed on the basis of previous work [27]. Concurrently, the computational complexity was also improved by adopting the "golden section search" [28]. Simulation results showed that the proposed scheme achieved a promising performance, which was comparable to that of OFDM in the absence of ICI.

Although much research is available in the literature related to CFO estimation and compensation, few schemes have been presented for time-varying CFO (TVCFO) estimation in underwater acoustic communication. Based on the above analysis, relative motion causes a Doppler effect or CFO, and a constant CFO can only be caused by a relatively uniform motion. However, in a complex and changeable underwater environment, it is difficult to guarantee a relatively uniform motion. Instead, an unpredictable acceleration often exists, which leads to a TVCFO in OFDM. This TVCFO is very difficult to deal with because its tracking and equalization usually require high computational complexity [29], which tends to increase linearly with the number of symbols in the OFDM frame. An introduction to the existing research is given below.

Mason et al. proposed a method for estimating the constant Doppler shift or slowly changing the time-varying Doppler shift within the packet by transmitting two identical OFDM symbols and employing a bank of parallel autocorrelators at the receiver [30]. This work was extended by Parrish et al. [31], who suggested tracking the Doppler variation with the help of marginal maximum likelihood estimation between symbols. Carrascosa et al. [32] proposed a TVCFO estimation method that predicted and tracked the nonuniform Doppler shift between adjacent data blocks based on the frequency and time correlation. Abdelkareem [29] assumed that the Doppler shift varied linearly among OFDM symbols, based on the principle that a Doppler shift changes the signal length

in the time domain. This requires frequent sampling and interpolation to estimate and compensate for the Doppler shift within the duration of a symbol. Simultaneously, the first-order statistics of the cyclic prefix are also estimated to reduce the ICI. In 2016, Abdelkareem studied the effect of sudden changes in the acceleration and velocity directions on the cyclic prefix correlation and proposed an adaptive time-varying Doppler estimation scheme. This adaptive mechanism was embedded in the automatic selection of the best estimation method based on CP window center positioning, first-order expectation, and autocorrelation of the CP [33]. Avrashi first studied the closed-form expression of the received signal that passed through a double-spread channel based on the least squares criterion. The value of the constant CFO was obtained using a root-based and eigenvalue decomposition-based CFO estimator [25]. In 2022, Avrashi extended the constant CFO to a polynomial and piecewise model variation over time [9], and implemented a method for estimating the TVCFO based on previous research. Compared with a grid search, which imposes a high computational burden on a modem [33], heuristic-based intelligent optimization algorithms have remarkable advantages, including greater adaptability and higher solution efficiency [34]. Therefore, they have allowed great progress in channel estimation [35–39].

The differential evolution (DE) algorithm is a prevalent example of intelligent optimization algorithms. It has a simple structure with few parameters, but exhibits excellent performance [35,37]. The DE algorithm has a feature that distinguishes it from other intelligent optimization algorithms: it is especially suitable for solving problems where there are dependencies between the adjacent variables to be optimized [40,41]. The dependencies refer to the fact that variables are linked by a similar influencing factor, such as Rosenbrock, Schaffer F7, and Whitley's composite functions in the benchmark suites. Coincidentally, underwater acoustic channel conditions do not change suddenly under normal circumstances. Even when the CFO changes over time, the CFO value on a subsequent block changes on the basis of the previous CFO value in terms of the OFDM structure. In other words, time-varying CFO estimation for OFDM systems falls squarely into the category of problem optimization with adjacent variables depending. In summary, the specific mutation and crossover operations of the DE algorithm can be used to track the time-varying CFO values of adjacent blocks in an OFDM data frame. After a limited number of iterations, the best estimate of the time-varying subcarrier frequency offset can be obtained.

From the literature, an OFDM model analogous to the MC-CDMA system can realize perfect ICI cancellation without losing any system overhead [26,27]. Considering the significant advantages and development potential of this scheme in underwater acoustic communication, we extended the model to time-varying environments and obtained a TVCFO estimation and thus compensation in this study. Simultaneously, the crossover characteristic of the DE algorithm was used to track the TVCFO and obtain the best estimation values based on its strong optimization ability. Specifically, the CFO value of each block was regarded as a variable to be optimized in the DE. The spread code matrix in the MC-CDMA system was obtained based on the variables by analogy, and then the received signal was reconstructed using the estimated CFO values. The Euclidean distance between the reconstructed and received signals was used to form the cost function. The optimal estimation of the TVCFO was achieved by the iterative use of the genetic operators of the DE.

The objective of this investigation was to study the performance of time-varying CFO estimation in OFDM systems based on the DE algorithm due to its advantages in solving problems with adjacent variables depending. The main contribution of this paper is to provide a feasible idea for time-varying CFO estimation, and the proposed method not only has the general applicability of modulation methods but also can improve the noise tolerance in demodulation. The remainder of this paper is organized as follows: Section 2 introduces the OFDM system model and DE. Section 3 details the proposed OFDM TVCFO estimation methods. The results and discussion are presented in Section 4. Finally, we conclude this paper and make suggestions for future research in Section 5.

2. Methodology

This section discusses the principle that allows the OFDM with ICI to be regarded as an MC-CDMA system on the receiver side, which is the basis for the CFO estimation. The DE algorithm is introduced, and the reasons why it is suitable for dealing with problems involving dependencies between adjacent variables are emphasized.

2.1. CFO Estimation in OFDM System with ICI

Assume that the OFDM system used for the analysis below has N subcarriers. When $H(k)$ denotes the complex channel frequency response on the k-th received subcarrier, the channel fading diagonal matrix is $\mathbf{\Lambda} = diag(H(0), H(1), \ldots, H(N-1))$. Received OFDM block symbol $\mathbf{Y}$ with a CFO is represented as follows:

$$\mathbf{Y} = \mathbf{X\Lambda S} + \mathbf{W}, \tag{1}$$

where $\mathbf{S}$ denotes transmitted block symbols, and $\mathbf{W}$ represents the additive white Gaussian noise vector. $\mathbf{S}$ represents an $N \times N$ ICI matrix. The specific elements can be represented by the following formula :

$$\mathbf{S} = \begin{bmatrix} S(0) & S(-1) & \cdots & S(1-N) \\ S(1) & S(0) & \cdots & S(2-N) \\ \vdots & \vdots & \ddots & \vdots \\ S(N-1) & S(N-2) & \cdots & S(0) \end{bmatrix}_{N \times N}. \tag{2}$$

The element in the p-th row and q-th column of the $\mathbf{S}$ matrix is $S_{p,q} = S(p-q)$, which is calculated in the following form:

$$S_{p,q} = \frac{\sin(\pi(p-q+\varepsilon))}{N\sin(\pi(p-q+\varepsilon)/N)} e^{j\pi\frac{(p-q+\varepsilon)(N-1)}{N}}, \tag{3}$$

where $\varepsilon = \Delta F/\Delta f$ represents the normalized CFO calculated using the CFO ΔF and subcarrier spacing Δf.

According to (1), the OFDM received symbol with CFO can be regarded as the MC-CDMA system [26,27]. Therefore, the received $k-$th data symbol can be considered as the $k-$th vector to form the spreading code matrix. By performing eigenvalue decomposition on the $\mathbf{S}$ matrix, the following relationship can be obtained:

$$\mathbf{S} = \mathbf{F}^{\mathrm{H}}\mathbf{\Phi}(\varepsilon)\mathbf{F}, \tag{4}$$

where $\mathbf{\Phi}$ is a diagonal matrix containing the CFO information, with the $n-$th element of $\mathbf{\Phi} = \mathrm{diag}(\phi_0, \phi_1, \cdots, \phi_{N-1})$ defined as $\phi_n = e^{j2\pi\varepsilon n/N}$. Matrices $\mathbf{F}$ and $\mathbf{F}^H$ denote the normalized discrete Fourier transform matrix and its conjugate transpose, respectively. The element in the $m-$th row and $n-$th column of matrix $\mathbf{F}$ can be expressed as $F_{m,n} = \frac{1}{\sqrt{N}}e^{-j2\pi/K \cdot mn}$. It can be proven that matrix $\mathbf{S}$ is an orthogonal matrix:

$$\begin{aligned} \mathbf{S}\mathbf{S}^{\mathrm{H}} &= \left(\mathbf{F}^{\mathrm{H}}\mathbf{\Psi}(\varepsilon)\mathbf{F}\right)\left(\mathbf{F}^{\mathrm{H}}\mathbf{\Psi}(\varepsilon)\mathbf{F}\right)^{\mathrm{H}} \\ &= \left(\mathbf{F}^{\mathrm{H}}\mathbf{\Psi}(\varepsilon)\mathbf{F}\right)\left(\mathbf{F}^{\mathrm{H}}\mathbf{\Psi}(-\varepsilon)\mathbf{F}\right) = \mathbf{I}. \end{aligned} \tag{5}$$

Based on the above description, when there is ICI caused by the CFO, the received OFDM symbols have expressions similar to that of the orthogonal MC-CDMA system. Therefore, the OFDM with ICI can be regarded as an orthogonal MC-CDMA system based on the spreading code matrix $\mathbf{S}$. If the vector of received OFDM symbols $\mathbf{Y}$ is processed by the conjugate transpose matrix of spreading code matrix $\mathbf{Y}$ and the inverse channel fading diagonal matrix $\mathbf{\Lambda}^{-1}$, we can deduce the explicit expression between the results and vector of transmitted symbols $\mathbf{X}$:

$$\boldsymbol{R} = \boldsymbol{Y}\boldsymbol{S}^{\mathrm{H}}\boldsymbol{\Lambda}^{-1} = \boldsymbol{X} + \boldsymbol{W}\boldsymbol{S}^{\mathrm{H}}\boldsymbol{\Lambda}^{-1}. \tag{6}$$

where $\boldsymbol{W}\boldsymbol{S}^{H}$ and $\boldsymbol{W}$ have the same covariance matrix because $\boldsymbol{S}^{H}$ is also an orthogonal matrix. The estimated values of transmitted symbol vector $\boldsymbol{X}$ can be obtained by performing the decision of $\boldsymbol{R}$, that is $\hat{\boldsymbol{X}} = D(\boldsymbol{R})$, where $D(\cdot)$ represents the decision function. Subsequently, the received signal can be reconstructed as $\hat{\boldsymbol{Y}}$ with $\hat{\boldsymbol{X}}$ and ICI coefficient matrix $\boldsymbol{S}(\hat{\varepsilon})$:

$$\hat{\boldsymbol{Y}} = \hat{\boldsymbol{X}}\boldsymbol{\Lambda}\boldsymbol{S}(\hat{\varepsilon}). \tag{7}$$

When the CFO is correctly estimated and compensated, the estimated values of the received signals are equal to the received signals without the influence of noise $\hat{\boldsymbol{Y}} = \boldsymbol{Y}$. Therefore, a smaller difference between the reconstructed and received signals ($\hat{\boldsymbol{Y}}$ and $\boldsymbol{Y}$, respectively) indicates that the estimated CFO, $\hat{\varepsilon}$, is closer to the actual CFO. The Euclidean distance between the received and reconstructed signals can be used to measure the difference between them:

$$\begin{aligned} J(\hat{\varepsilon}) =& \|\hat{\boldsymbol{Y}} - \boldsymbol{Y}\|^2 = \|\hat{\boldsymbol{X}}\boldsymbol{\Lambda}\boldsymbol{S}(\hat{\varepsilon}) - \boldsymbol{Y}\|^2 \\ =& \|D(\boldsymbol{R})\boldsymbol{\Lambda}\boldsymbol{S}(\hat{\varepsilon}) - \boldsymbol{Y}\|^2 \\ =& \left\|D\left(\boldsymbol{Y}\hat{\boldsymbol{S}}^{\mathrm{H}}(\hat{\varepsilon})\boldsymbol{\Lambda}^{-1}\right)\boldsymbol{\Lambda}\boldsymbol{S}(\hat{\varepsilon}) - \boldsymbol{Y}\right\|^2. \end{aligned} \tag{8}$$

Therefore, the optimal CFO value, $\hat{\varepsilon}$, can be obtained by minimizing the cost function, $J(\hat{\varepsilon})$:

$$\hat{\varepsilon} = \arg\min(J(\hat{\varepsilon})). \tag{9}$$

A flowchart that describes how to execute the CFO estimation of the OFDM system with ICI is shown in Figure 1.
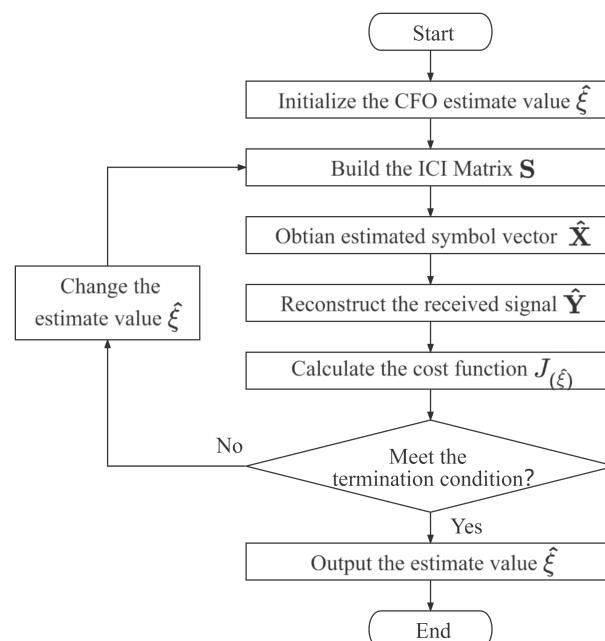

Figure 1. A flowchart that describes the process of the CFO estimation presented in Section 2.1.

2.2. Introduction to the DE Algorithm

This subsection briefly outlines the principles for optimizing a problem using heuristic algorithms, along with the mechanism of the DE algorithm. In general, an unconstrained single-objective optimization problem with n decision variables can be described as follows:

$$
\begin{cases}
\textbf{minimize}: y = f(\boldsymbol{x}) \in \boldsymbol{Y} \\
\text{x} = [x_1, x_2, \ldots, x_n]^T \in \boldsymbol{X} \\
\quad l_j \leq x_j \leq u_j,
\end{cases}
\tag{10}
$$

where $\boldsymbol{x}$ is the vector of variables to be optimized, **y** is the function value corresponding to $\boldsymbol{x}$, $\boldsymbol{Y}$ is the objective space, **X** is a search space consisting of the boundaries of the variables in all dimensions, and u_j and l_j are the upper and lower bounds of the j-th optimization variable, respectively.

The DE algorithm is a population-based stochastic search algorithm. It encodes the population using Np d—dimensional vectors, where a single d—dimensional vector is called an individual whose elements are the variables to be optimized. The individual mentioned above is actually the solution to the optimization problem. The population initialization operation is followed by three genetic operations: mutation, crossover, and selection. The genetic operation is repeatedly executed until the stop condition is met. When the iterative process stops, the optimal solution is output. The mutation operation is a representative genetic operator of DE, and the algorithm is named after it. The mutation employs a scaled difference vector of terminal solutions to perturb a base vector [40]. The terminal and base vectors are randomly selected from the current population during the DE. There is a multitude of mutation strategies that differ from each other mainly by the number of differential vectors and construction of the base vector.

The goal when using the crossover operation in DE is to increase the population diversity [40]. Specifically, the crossover is used to generate trial vectors whose elements come from either the objective vector or mutation vector. There are two commonly used crossover operations in DE, namely, binomial crossover and exponential crossover. The type of crossover determines the number and contiguousness of variables, which are inherited from their parents [41]. Binomial crossover is performed by comparing a random number and preset crossover factor Cr for each variable to select the source of inheritance. Therefore, it is effective in solving distributed problems where there is no relationship among variables. Exponential crossover is used to randomly designate a starting point. Then, a random number and Cr are compared one by one from the starting point until the relationship is not satisfied. Thus, the ending point is determined. The variables from the starting point to the ending point are inherited from the mutation vector, and the rest are from the parent vector. Therefore, the dependencies between variables and their neighbors persist, except for the start and end points. Thus, it is more suitable for solving adjacent problems where there is a dependency relationship between adjacent variables. In this study, an exponential crossover was used to track the CFO variation between adjacent symbols.

The selection operation was employed to select the promising vectors from the trial population and objective population, which became members of the objective population in the next generation. To be concrete, the trial vector was compared with the corresponding objective vector of the whole population in sequence. A vector with a smaller fitness value appeared in the next generation if the optimization problem was the minimization problem. Therefore, these vectors formed the population, which became the objective population in the next generation. The mutation, crossover, and selection operations were repeated in a loop until certain termination conditions were met. The individual with the best fitness was regarded as the optimal solution to the problem in the final population.

3. Time-Varying Carrier Frequency Offset Estimation

The previous section discussed a model OFDM system with ICI caused by the CFO, which was analogous to the orthogonal MC-CDMA was discussed. However, because of the complexity of underwater acoustic environments, it is inappropriate to assume that both transducers will maintain uniform motion over a long period. Their motion can be impacted by multiple factors, including sea surface undulation, turbulence, and internal wave motion. More often, this relative motion is a variable speed motion with random accelerations. Therefore, the ICI in the received OFDM signal has a TVCFO

rather than a constant CFO. In general, the duration of one OFDM block of underwater acoustic communication lasts from tens of milliseconds to approximately one hundred milliseconds. Considering the actual environment for underwater acoustic communication, we can reasonably assume that the acceleration of the relative motion is constant over the duration of an OFDM block; that is, the CFO changes within the duration of an OFDM frame but remains constant in the very short OFDM time block. Therefore, the model mentioned above should be modified slightly to change the constant CFO in the frame time to a variable value, while allowing it to remain steady during the block duration. The estimation of a single CFO value within a data frame is changed to finding the CFO values for each block within a data frame.

Water works as a waveguide in communication; however, it is also a viscous fluid, making it impossible for channel conditions to change quickly. Therefore, there are dependencies between the CFO values in neighboring blocks of the received signal because the velocity of relative motion corresponding to the latter time block changes based on that of the previous time block, which is adjacent to it. As previously mentioned, relevant research has shown that the DE algorithm is particularly suitable for dealing with problems in which there are dependencies between the adjacent parameters to be optimized. Therefore, we used the DE algorithm to jointly optimize the estimated TVCFO values in each block of the received signal. Based on the above analysis, the specific steps for estimating the TVCFO using the DE algorithm are given below.

(1)   Determine optimization variables and their limits

Based on the previous analysis, this study investigated TVCFO estimation, where the CFO values on multiple OFDM symbol blocks varied over time and were unequal. The CFO on each OFDM symbol in a frame can be regarded as a variable to be optimized. If a data frame has N symbol blocks, then the $i-$th individual of the DE can be expressed as follows:

$$\varepsilon_i = (\varepsilon_{i,1}, \ \varepsilon_{i,2}, \ \ldots, \ \varepsilon_{i,N}) \tag{11}$$

for $i = 1, 2, \ldots, Np$, where Np is the population size of the DE. According to the introduction of Formula (3), the normalized CFO is in the range of [0, 1]. In other words, the minimum value, ε_{min}, is 0, and the maximum value, ε_{max}, is 1. If it exceeds the limit, it should be readjusted back to this range; otherwise, it is meaningless. Real number DE coding was adopted in this study.

(2)   Determine the fitness function

The fitness function can generally be regarded as a cost function in an optimization problem or its equivalent transformation and is mainly used for measuring the quality of solutions. For minimization problems, a smaller fitness function value indicates a higher quality for the individual solution. When the fitness function value is zero, the solution has the highest quality, and the individual is therefore the optimal solution. When the optimal solution was introduced and the Euclidean distance between the reconstructed and received signals was zero, the estimated value of the CFO was the actual value of the received OFDM signal. Although the fitness value could not be zero because of the influence of noise, there was still a relationship between the quality of the solution and its fitness. A smaller fitness value indicated that the estimated value of the CFO was closer to the real value. Because the TVCFO was considered, it was necessary to take the overall performance of the CFO values on all the symbol blocks within an OFDM frame into account. Hence, the mean value of the reconstruction differences was employed as the fitness value:

$$f(\hat{\varepsilon}) = \text{mean}(J(\hat{\varepsilon})), \tag{12}$$

where $\hat{\varepsilon}$ denotes the vector of the estimated CFO values on each block.

(3)   Initialize the population

The initial population, $\mathbf{P}^0$, consists of Np original individuals, which are randomly generated in the decision space constrained by the upper and lower bounds of each dimension:

$$\begin{aligned} \boldsymbol{\varepsilon}_{\min} &= \left[\varepsilon_{\min,1},\ \varepsilon_{\min,2},\ \ldots,\ \varepsilon_{\min,N}\right]^T \\ \boldsymbol{\varepsilon}_{\max} &= \left[\varepsilon_{\max,1},\ \varepsilon_{\max,2},\ \ldots,\ \varepsilon_{\max,N}\right]^T. \end{aligned} \tag{13}$$

Thus $\mathbf{P}^0$ can be expressed as follows:

$$\mathbf{P}^0 = \left\{ \boldsymbol{\varepsilon}_i^0 = \left(\varepsilon_{i,1}^0, \varepsilon_{i,2}^0, \ldots, \varepsilon_{i,N}^0\right) \right\} \tag{14}$$

for $i = 1,\ 2,\ \ldots,\ Np$. In addition, the fitness value of the population can be obtained by substituting the initial population into the fitness function (12).

(4)   Perform genetic operations:

Populations are sorted based on the fitness values in the typical method before performing genetic operations. The sorting operation is used to facilitate the mutation operator to make full use of promising individuals with high quality because a solution with higher quality is the individual that carries more useful information. In other words, these individuals can accelerate the convergence and guide the population to find the optimal solution faster.

After completing the sorting operation, the mutation operation is performed. This operation can be expressed by the following formula:

$$\boldsymbol{\xi}_i^g = \boldsymbol{\varepsilon}_i^g + f_0 \cdot \left(\boldsymbol{\varepsilon}_{pbest}^g - \boldsymbol{\varepsilon}_i^g\right) + f_0 \cdot \left(\boldsymbol{\varepsilon}_{r1}^g - \boldsymbol{\varepsilon}_{r2}^g\right) \tag{15}$$

where $\boldsymbol{\xi}_i$ is the mutation vector corresponding to the i-th target vector, $\boldsymbol{\varepsilon}_i$. $\boldsymbol{\xi}_i$ is a promising individual selected from the top $p\%$ of the current population. Individual $\boldsymbol{\varepsilon}_{r1}$ is randomly selected from the current population, while individual $\boldsymbol{\varepsilon}_{r2}$ comes from the union of the current population and these obsolete individuals, which can increase the diversity and prevent mutation vector $\boldsymbol{\xi}_i$ from falling into the local optima. These vectors differ from each other. Mutation factor f_0, which usually lies in the range of $[0, 1]$, is used to scale the difference vector. Here, g represents the g-th generation of genetic operations.

Following the mutation, an exponential crossover operation is performed on mutation vector $\boldsymbol{\xi}_i$ and objective vector $\boldsymbol{\varepsilon}_i$ to further increase the diversity of the current population. Specifically, integer r is randomly selected from $[1, N]$. This integer acts as the starting point of the offspring vector, from which it is exchanged with the components of the mutation vector. Another integer L limited by $[1, N]$ is used to determine the dimension proportion of the offspring inherited from the mutation vector. L can be determined using the following pseudocode:

$$\begin{aligned} & L = 0; \\ & \text{do } \{ \\ & \quad L = L + 1; \\ & \} \text{ While } ((\text{ rand } [0,1) < Cr) \ \& \ (L \leq N)). \end{aligned} \tag{16}$$

Crossover rate Cr is a parameter that controls the value of L. After parameters r and L are determined, the offspring vector can be obtained as follows:

$$\varsigma_{i,j}^g = \begin{cases} \xi_{i,j}^g & \text{if } j = \langle r, \ldots, r+L-1 \rangle_N, \\ \varepsilon_{i,j}^g & \text{otherwise} \end{cases} \tag{17}$$

where $\langle \cdot \rangle$ is an operation that obtains the remainder. Next, the offspring are evaluated.

Lastly, the selection operation is executed. For a minimization optimization problem, the individuals with lower fitness values in the parents and offspring survive to the next generation. Then, a new population is obtained. The selection operation is as follows:

$$\varepsilon_i^{g+1} = \begin{cases} \varsigma_i^g & \text{if } f\left(\varsigma_i^g\right) \leq f\left(\varepsilon_i^g\right) \\ \varepsilon_i^g & \text{otherwise} \end{cases}, \tag{18}$$

where $f(\cdot)$ represents the fitness value of the corresponding vector, (i.e., the function value of the cost function); ς_i represents the offspring individuals; and ε_i represents the parent individuals.

(5) Judge termination conditions

There are two main types of termination conditions: when the error accuracy of the best solution reaches a pre-set value and when the maximum iteration number meets a pre-set value according to the computing complexity. If the termination conditions are met, the individual corresponding to the best quality is output as the optimal solution in this loop. Otherwise, the execution is repeated from step 4 until the termination conditions are met.

Algorithm 1 presents the pseudocode of the proposed DE-aided TVCFO estimation.

Algorithm 1 Pseudocode of the proposed scheme

Step 1 Initialization

Set population size Np, dimension N, maximum generation number g_{max}, and generation counter $g = 0$. Then initialize the original population $\boldsymbol{P}^0 = \left\{ \varepsilon_1^0, \varepsilon_2^0, \ldots, \varepsilon_N^0 \right\}$ with $\varepsilon_i = (\varepsilon_{i,1}, \varepsilon_{i,2}, \ldots, \varepsilon_{i,N})$ uniformly distributed in the limits, and evaluate the original population.

Step 2 Evolution Iteration
WHILE ($g \leq g_{max}$) DO
    Step 2.1 Preparation
    Sort current population $\boldsymbol{P}^g$ according to the fitness values;
    Step 2.2 Mutation Operation
    Determine the value of mutation factor f_0;
    Perform the mutation operation according to (15);
    Step 2.3 Crossover Operation
    Determine the crossover rate Cr in the type of exponential crossover;
    Execute the crossover operation based on (17) to obtain the offspring;
    Step 2.4 Selection Operation
    Substitute the offspring into (12) and get the fitness value;
    Carry out the selection operation according to (18);
    Step 2.5 Update the Generation Counter
    Increase the generation counter by 1, that is $g = g + 1$;
END WHILE
Step 3 Output the Solution
Solution with the smallest fitness value is output as the best TVCFO estimation.

---

4. Results and Discussion

This section first describes a simulation experiment that used the proposed method for TVCFO estimation. Then the results are analyzed. To verify the suitability of using DE to estimate the TVCFO in an OFDM system, it was compared with representative intelligent optimization algorithms applied to channel estimation (the genetic algorithm (GA) [39] and Simulated Annealing Mutated-Genetic Algorithm (SAMGA) [36]) on the same model. We gathered the statistics and results of the proposed scheme, as well as the received signal with and without the actual TVCFO compensation, using the bit error rate (BER). Finally, the performances of the proposed scheme for four different modulation types were examined given to test its universality.

An OFDM system with eight blocks in one frame was considered. Each block contained $k = 64$ subcarriers. Binary phase-shift keying (BPSK) modulation was adopted if there was no additionality specified. A channel fading diagonal matrix was obtained based on the channel impulse response, as discussed in [33] (i.e., $h(n) = 0.6708\delta(n) + 0.5\delta(n-1) + 0.3873\delta(n-2) + 0.3162\delta(n-3) + 0.2236\delta(n-4)$) [33]. Two different types of TVCFO were considered for simulation analyses i.e., fourth-order polynomial function and sinusoidal function [9]. One of the CFO variations was a fourth-order polynomial function (19):

$$
\epsilon[n] = \sum_{l=0}^{\infty} \epsilon_l n^l, \quad 1 \le n \le K
$$
$$
b_l = K^l \epsilon_l,
$$

(19)

where b_l are uniformly distributed and randomly taken from the limits of $[-0.25, 0.25]$, that is $b_l \sim \mathcal{U}[-0.25, 0.25]$, and K is the number of blocks. The other variation form was the sinusoidal function (20) :

$$
\epsilon(n) = \Delta f \left[A_0 + A \sin\left(2\pi n \frac{f_{\sin}}{K} \right) \right],
$$

(20)

where $A_0, A \sim \mathcal{U}[-0.25, 0.25]$ and $f_{sin} \sim \mathcal{U}[0.25, 2]$. The limits of the TVCFO estimation values were modified as $[-0.5, 0.5]$ for convenience.

4.1. Results of Different Estimators

Based on a model where the received OFDM signal with ICI caused by the TVCFO was analogous to the orthogonal MC- CDMA system, the estimation was conducted using DE. To verify its suitability for considering the dependencies between the CFO values in adjacent blocks of the OFDM data frame, the performance of the DE algorithm for the TVCFO estimation was compared with those of the SAMGA [36] and GA [39], which are frequently used in channel estimation. The parameters of the DE algorithm used in this study were consistent with those in [42], and the parameters of the compared algorithms were set to the values reported in the original papers.

Figure 2 shows the performances of the DE algorithm, GA, and SAMGA when estimating the TVCFO in the form of a polynomial function with the same computing resources. The data in the figure are the averages obtained from 50 independent runs under different SNRs, as are the data in the following figures. The measurements show the Root-Mean-Square Error (RMSE) of the CFO values on the OFDM blocks, which can be defined as follows:

$$
\text{RMSE}(\hat{\varepsilon}) = \sqrt{\frac{1}{K} \sum_{i=1}^{K} (\hat{\varepsilon}_i - \varepsilon_i)^2}.
$$

(21)

The black, blue, and red curves represent the results obtained by the SAMGA, GA, and DE estimators for the improved model, respectively. The RMSE values improved as the SNR increased. However, the SAMGA did not improve the performance of the genetic algorithm in this case. It was inferred that this lack of improvement was a result of the limited computing resources, which made the large population size unsuitable. Moreover, the SAMGA increased the diversity to prevent premature, which also wasted computing resources. Generally, the available time resources are seriously constrained in underwater acoustic communication. Therefore, the advantages of the SAMGA could not be fully utilized. The GA had a remarkable performance compared to that of the SAMGA; However, the performance of the DE algorithm was slightly better than that of the GA. The average RMSE value with the DE algorithm was approximately 9.68% smaller than that of the GA when the SNR was less than 12 dB. When the SNR exceeded 12 dB, the average RMSE of the DE estimator increased, becoming 30.02% smaller than that of the GA estimator, and finally reaching a peak that was 43.71% lower at 20 dB. This significant improvement was due, not

only to the adaptive parameters of the DE algorithm used in this study [42], but also to its advantage when solving problems with dependencies between adjacent variables. The GA could not compete with the DE algorithm in terms of the dependencies between adjacent variables which is the pivotal characteristic of TVCFO estimation. The above analysis was confirmed by the gap between the two curves becoming progressively obvious as the SNR increased. Because the amplitude of the noise followed a normal distribution and had significant randomness, the dependencies between adjacent variables were diluted. However, as the SNR increased, the influence of the noise decreased, and the connections between adjacent TVCFO values could be more easily mined by the DE algorithm.

Figure 2. Performances of three estimators on the improved model with CFO values varying in polynomial function.

The best results of the three estimators were substituted into the improved system model for demodulation. The BER values were determined based on the demodulation results, and are summarized in Figure 3. According to the curve, when the SNR did not exceed 13 dB, the performances of the three estimators were comparable, and it may be inferred that their accuracies were acceptable. Under the condition of a low SNR, the source of the error values was mainly the noise, and the CFO estimation bias was relatively negligible. The difference between the three estimators becomes clear from the results at 14 dB. When the SNR is less than 17 dB, the performance of the SAMGA estimator is comparable to those of the GA and DE estimators. After the SNR exceeds 17 dB, the SAMGA with the lowest estimation accuracy shows the worst demodulation performance. The comparison between GA and DE algorithms fluctuated, which was a result of the combined effect of noise and the CFO estimation accuracy. The noise uncertainty led to a performance undulation with the same SNR for both estimators. With an increase in the number of result statistics or SNR, the gap between the DE and GA estimations became apparent, as was evidenced by the results at 20 dB.

The results of the three algorithms when the CFO values varied in the form of a sinusoidal function with the same computing times are shown in Figure 4. By comparing the data in Figures 2 and 4, similar conclusions can be drawn: the estimation accuracy of the DE algorithm was significantly better than those of the SAMGA and GA. The mismatch between population size and mutation operation adopted by the SAMGA for the TVCFO estimation caused it to have the worst performance of the three estimators. In addition, it should be noted that for the SAMGA estimation, the RMSE of the CFO value with the sinusoidal function was roughly an order of magnitude worse than that in the polynomial function. The difference in the estimation accuracy also led to distinct demodulation results. As seen by the BER statistics for the SAMGA estimator in Figure 5, the demodulation results were almost unacceptable because of the large deviation in the CFO estimation. Additionally, the CFO estimation bias of the SAMGA estimator fluctuated very little for different SNRs. Therefore, the BER improvement seen in Figure 5 came

merely from the increase in the SNR. The BER curves for the GA and DE estimators further corroborated the conclusions we drew above: the demodulation performances of the DE and GA estimators were dominated by the SNR in the cases with low SNRs, whereas under high SNR conditions, the quality of the TVCFO estimation was reflected in the BER results. The RMSE of the DE estimator was 36.13% smaller than that of the GA estimator when the SNR was 20 dB, which corresponded to a 75% improvement in the BER after demodulation. Based on an analysis of the results of the simulation experiments with the three estimators using two different variations of CFO values, we can safely conclude that, because the dependencies between adjacent variables were considered by the DE algorithm and not the other intelligent optimization algorithms (the GA and SAMGA), it would be appropriate to use the DE algorithm to estimate the TVCFO in underwater acoustic communication.
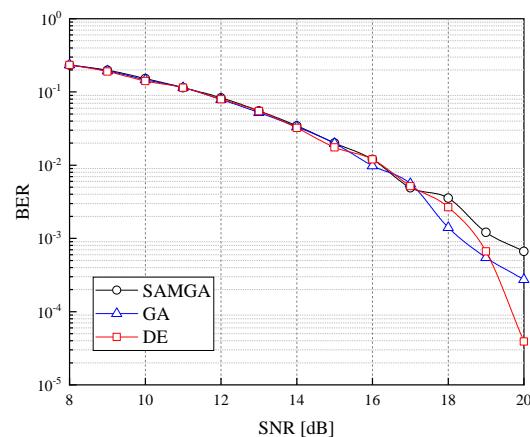

Figure 3. Bit error rate statistics of three estimators on the improved model with CFO values varying as a polynomial function.
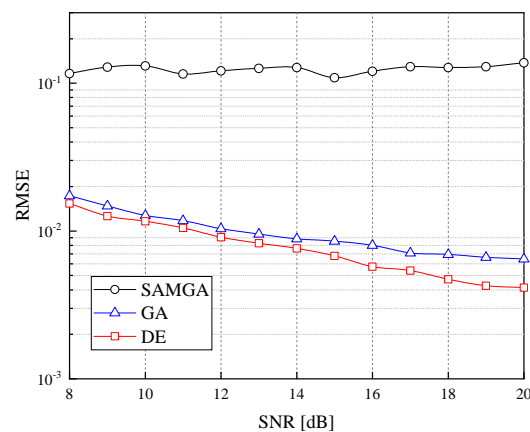

Figure 4. Performances of three estimators on the improved model with CFO values varying as a sinusoidal function.
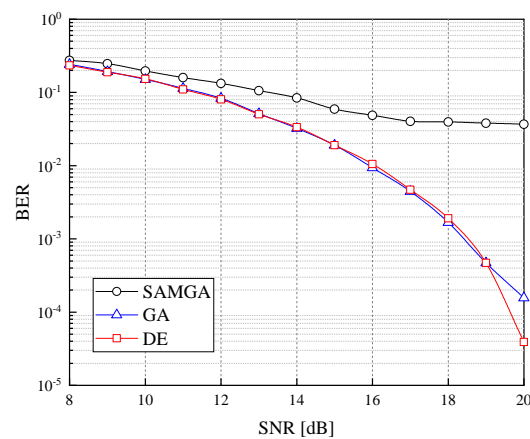
Figure 5. Bit error rate statistics of three estimators on the improved model with CFO values varying as a sinusoidal function.

4.2. Results of Demodulation with/without Compensation

To further verify the performance of the DE estimator of the TVCFO, the demodulation results with and without CFO compensation and with DE estimation value compensation are given in Figure 6. In this figure, the black solid line with a circle represents the demodulation results for the OFDM system model without compensation. The blue dashed line which is marked as "OFDM without TVCFO" shows the demodulation results in the absence of the CFO, which is equivalent to compensation with real CFO values. And the red squares marked as "OFDM with TVCFO compensation" show the demodulation results when using the DE estimation values. The BER without compensation was much higher than that with compensation, which was predicted. Surprisingly, the results of the compensation with the estimated values were highly coincident with the results when there were no CFO values. Moreover, the demodulation results for the CFO compensation with DE estimation were better than those without the CFO when the SNR is equal to 20 dB. The only possible reason for this was the influence of noise. According to (7) and (8), the reconstructed signal could be used to directly calculate the cost function with the actual received signal without considering the noise. Therefore, the effect of noise on the demodulation performance was converted into the CFO on each OFDM block by the DE estimator and taken into account in the simulation values.
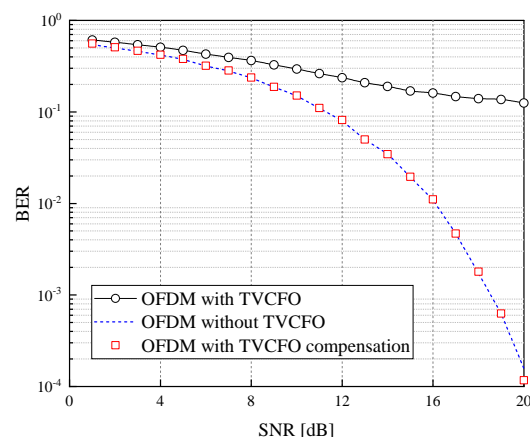

Figure 6. Bit error rate statistics of demodulations in three cases: without CFO compensation, with actual CFO compensation, and with DE estimation values compensation.

Figure 7 shows a constellation map after demodulation in the three cases: without the CFO compensation, with the actual CFO compensation, and with the DE estimation value compensation. The CFO values that varied as a sinusoidal function were adopted in these simulations. The received data without CFO compensation were randomly distributed,

which resulted in difficulties in making the correct decision. In the case of the compensation with the DE estimation values, the data surrounding the correct constellation points were well organized. Importantly, the data boundaries were very clear, because valid decisions could be easily made. In addition, these data were highly coincident with the compensation results with the actual CFO values. Specifically, there is significant overlapping between the red square and blue star data in the figure. This phenomenon demonstrates the validity of the proposed scheme for estimating TVCFO values.
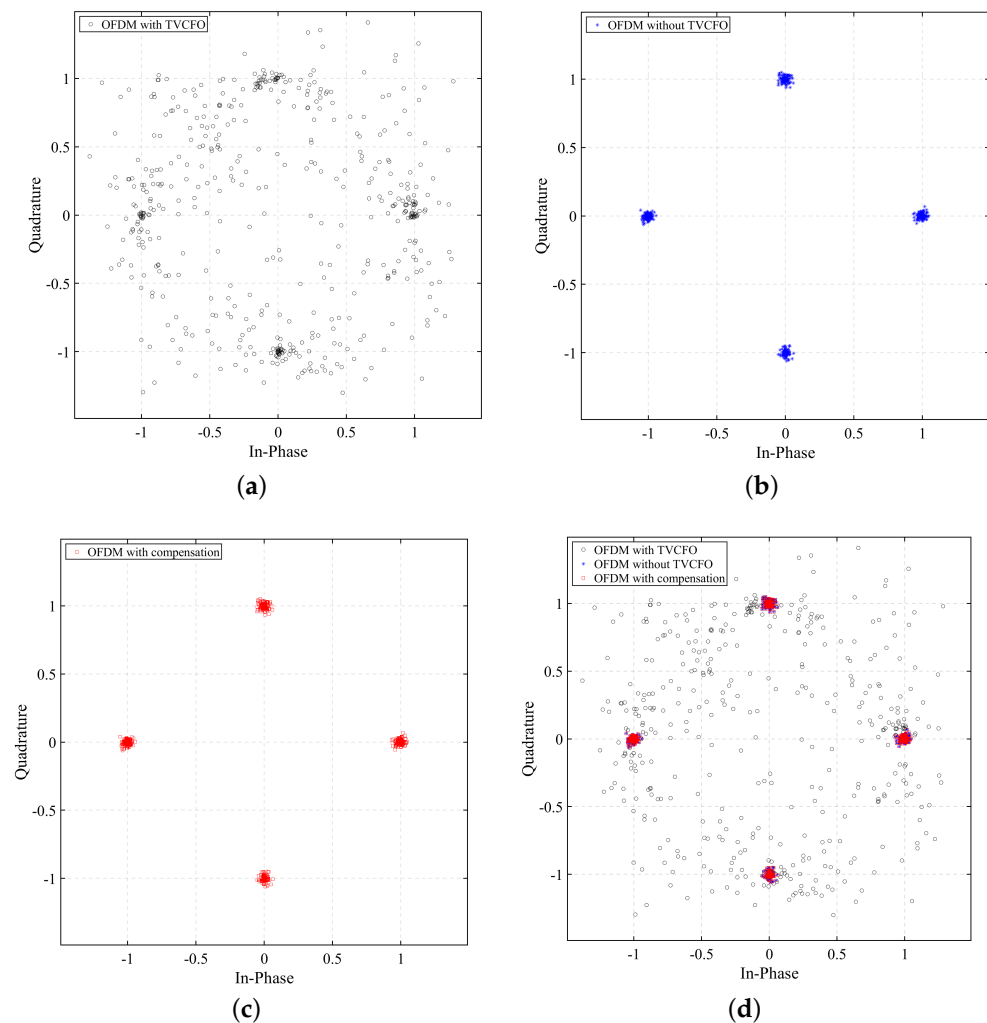

Figure 7. Constellations of demodulations in three cases: (**a**) without CFO compensation, (**b**) with actual CFO compensation, (**c**) with DE estimation values compensation and (**d**) comparison of the three.

4.3. Results of Different Modulations

Finally, we used the proposed scheme with four modulation methods to investigate the performance in terms of its universality. The BER values of the demodulation results were calculated and are shown in Figure 8. The four different modulation methods were BPSK, quadrature phase-shift keying (QPSK), differential QPSK (DQPSK), and 16-bit quadrature amplitude modulation (16QAM). According to the data, the demodulation results with 16QAM were similar to those of the QPSK cases analyzed above. The DE algorithm was used to estimate the CFO value for each OFDM block before the received signal was compensated with the values. A comparison of the curves shows that its demodulation was significantly better than the case of direct demodulation without compensation. Moreover, the compensation results with the DE estimated values were consistent with those obtained using actual CFO values. This means that the actual TVCFO value could be obtained

using the DE estimator. In the case of BPSK, the DE algorithm with estimation value compensation performed better than that without the TVCFO, which was clear in the high SNR situation. This was because there was less pressure to make a correct BPSK judgment compared to QPSK with the same estimation accuracy, which was affected by the fewer decision options of BPSK. The effect of noise on the OFDM block was considered to be part of the CFO. Therefore, the possibility of a mismatch was smaller because BPSK has fewer decision options. This was also the reason that the demodulation results based on the estimated values were slightly better. For DQPSK, the demodulation effect of the DE estimated values were worse than that of the compensation executed using the actual CFO values, which was also due to the effect of noise being regarded as carrier frequency deviation. Phase changes on adjacent subcarriers are employed to transmit information in the DQPSK modulation. However, the original information is destroyed by the equivalent CFO introduced when dealing with noise in the DE estimator. Therefore, the demodulation results deteriorated with the compensation of the actual TVCFO values. In general, it was relatively acceptable to use the DE algorithm to estimate the TVCFO in DQPSK. In summary, the TVCFO estimation using the DE algorithm was very effective in the PSK and QAM modulation modes. Although the performance of the DE algorithm in the DQPSK modulation mode was not the same as those with the PSK and QAM, the demodulation result after compensation based on the estimated value is significantly better than that without compensation. Moreover, as the SNR increases, the gain after compensation is also more obvious.
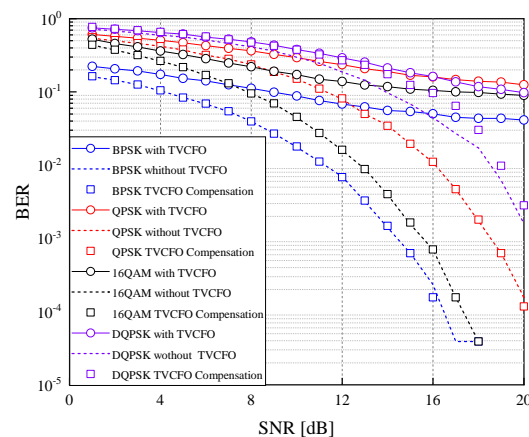

Figure 8. Bit error rate statistics of demodulation results in four cases: BPSK (blue), QPSK (red), DQPSK (purple), and 16QAM (black).

This section showed how three estimators (the SAMGA, GA, and DE algorithms) were adopted for the TVCFO estimation on the improved OFDM model. A comparison of the results in terms of the RMSE of the estimated values and the BER of demodulation showed that the mechanism of the DE algorithm, which considers the dependencies among adjacent variables, was very suitable for solving the TVCFO estimation problem. The demodulation performances for the received signal without compensation, with actual CFO values, and with estimated values obtained by the DE compensation were determined. The results demonstrated that the proposed scheme could achieve real TVCFO values, and the effect of noise on the demodulation could also be considered in the QPSK modulation. Ultimately, the performances of the DE estimator with four modulation schemes, BPSK, QPSK, DQPSK, and 16QAM, were tested. The proposed scheme correctly estimated the TVCFO values under the QPSK and 16QAM modulation. The performance under BPSK modulation was the best of the four, and it was easier to reduce the influence of noise under a high SNR. The DQPSK modulation was not as promising as the other three modulations. However, the results were also acceptable, and the DE estimator could be utilized with DQPSK and can be worked as a candidate.

5. Conclusions

Previous studies have shown that an OFDM signal with ICI on the receiver side can be regarded as an MC-CDMA system, in which the spreading code matrix is the ICI matrix. This study extended the system model to TV-CFO estimation. Meanwhile, intelligent optimization algorithms are frequently used for channel estimation, and the DE algorithm is a prevalent example. The DE algorithm has a unique feature in that its crossover operation is very suitable for solving problems in which there are dependencies between adjacent variables. Considering the change in the relative velocity of the sending and receiving terminals, which produces the TVCFO in the received signal, the velocity changes in different moments are linked by the acceleration. Therefore, the DE algorithm was employed to capture the dependencies between the CFO values on adjacent OFDM blocks. Simulation results showed that the performance of the DE algorithm was better than those of other intelligent optimization algorithms (the SAMGA and GA) in terms of the RMSE of the estimated CFO values and the BER of the demodulation. Furthermore, the proposed scheme not only achieved a demodulation performance with actual TVCFO values, but also reduced the demodulation deterioration caused by noise in both the PSK and QAM modulations. Future research could focus on the effect of noise on the DQPSK modulation with the DE estimator. The DE estimator could also be further utilized to achieve a better balance between the computational complexity and accuracy of TVCFO estimation.

Author Contributions: Conceptualization, H.W.; methodology, W.J. and Q.H.; software, H.W. and W.J.; validation, Q.H.; formal analysis, W.J.; investigation, W.J.; data curation, J.Z. and Y.J.; writing—original draft preparation, H.W.; writing—review and editing, J.Z. and Y.J.; visualization, Y.J.; supervision, Q.H. All authors have read and agreed to the published version of the manuscript.

Institutional Review Board Statement: Not applicable.

Informed Consent Statement: Not applicable.

Data Availability Statement: Not applicable.

Conflicts of Interest: The authors declare no conflict of interest.

References

1. Melki, R.; Noura, H.N.; Mansour, M.M.; Chehab, A. A survey on OFDM physical layer security. *Phys. Commun.* **2019**, *32*, 1–30. [CrossRef]
2. Murad, M.; Tasadduq, I.A.; Otero, P. Ciphered BCH Codes for PAPR Reduction in the OFDM in Underwater Acoustic Channels. *J. Mar. Sci. Eng.* **2022**, *10*, 91. [CrossRef]
3. Sun, Y.; Shen, H.; Du, Z.; Peng, L.; Zhao, C. ICINet: ICI-Aware Neural Network Based Channel Estimation for Rapidly Time-Varying OFDM Systems. *IEEE Commun. Lett.* **2021**, *25*, 2973–2977. [CrossRef]
4. Tasadduq, I.A.; Murad, M.; Otero, P. CPM-OFDM Performance over Underwater Acoustic Channels. *J. Mar. Sci. Eng.* **2021**, *9*, 1104. [CrossRef]
5. Zhan, Q.; Minn, H. New Integer Normalized Carrier Frequency Offset Estimators. *IEEE Trans. Signal Process.* **2015**, *63*, 3657–3670. [CrossRef]
6. Li, S.; Wang, P.; Wang, S.; Cong, Y.; Liu, J.; Cui, X. Doppler estimation based on linear interpolation for underwater acoustic communication. *Trans. Emerg. Telecommun. Technol.* **2022**, *33*, e4519. [CrossRef]
7. Zhou, S.; Wang, Z. *OFDM for Underwater Acoustic Communications*; John Wiley & Sons: Hoboken, NJ, USA, 2014.
8. Meng, Y.; Zhang, W.; Stuber, G.L.; Wang, W. Blind Fast CFO Estimation and Performance Analysis for OFDM. *IEEE Trans. Veh. Technol.* **2020**, *69*, 11501–11514. [CrossRef]
9. Avrashi, G.; Amar, A.; Cohen, I. Time-varying carrier frequency offset estimation in OFDM underwater acoustic communication. *Signal Process.* **2022**, *190*, 108299. [CrossRef]
10. Liu, T.; Jin, S.; Wen, C.K.; You, X. A Data-aided Compensation of Clipped OFDM Signals by Bayesian Learning Scheme. In Proceedings of the 2019 11th International Conference on Wireless Communications and Signal Processing (WCSP), Xi'an, China, 23–25 October 2019; pp. 1–5.
11. Martín-Vega, F.J.; Gómez, G. A Low-Complexity Pilot-Based Frequency-Domain Channel Estimation for ICI Mitigation in OFDM Systems. *Electronics* **2021**, *10*, 1404. [CrossRef]

12. Syrjälä, V.; Levanen, T.; Ihalainen, T.; Valkama, M. Pilot allocation and computationally efficient non-iterative estimation of phase noise in OFDM. *IEEE Wirel. Commun. Lett.* **2019**, *8*, 640–643. [CrossRef]
13. Fang, T.; Liu, S.; Ma, L.; Zhang, L.; Khan, I.U. Subcarrier modulation identification of underwater acoustic OFDM based on block expectation maximization and likelihood. *Appl. Acoust.* **2021**, *173*, 107654. [CrossRef]
14. Murad, M.; Tasadduq, I.A.; Otero, P. Pilot-Assisted OFDM for Underwater Acoustic Communication. *J. Mar. Sci. Eng.* **2021**, *9*, 1382. [CrossRef]
15. Nandi, S.; Pathak, N.N.; Nandi, A. A novel adaptive optimized fast blind channel estimation for cyclic prefix assisted space–time block coded MIMO-OFDM systems. *Wirel. Pers. Commun.* **2020**, *115*, 1317–1333. [CrossRef]
16. Jeon, H.G.; Kim, K.S.; Serpedin, E. An efficient blind deterministic frequency offset estimator for OFDM systems. *IEEE Trans. Commun.* **2011**, *59*, 1133–1141. [CrossRef]
17. Liu, M.; Li, B.; Ge, J. Blind estimation for OFDM fractional frequency offset over multipath channels. *Wirel. Pers. Commun.* **2014**, *79*, 119–130. [CrossRef]
18. Lin, T.C.; Phoong, S.M. A new cyclic-prefix based algorithm for blind CFO estimation in OFDM systems. *IEEE Trans. Wirel. Commun.* **2016**, *15*, 3995–4008. [CrossRef]
19. Wang, H.; Yin, Q.; Feng, A. Low complexity blind frequency offset estimation based on downsampling for OFDM systems. In Proceedings of the IEEE GLOBECOM 2007-IEEE Global Telecommunications Conference, Washington, DC, USA, 26–30 November 2007; pp. 2831–2835.
20. Tai, W.J.; Pan, Y.C.; Phoong, S.M. A simple LS algorithm for improving ESPRIT-based blind CFO estimations in OFDM systems. In Proceedings of the IEEE International Symposium on Personal Indoor & Mobile Radio Communications, Sydney, Australia, 9–12 September 2012.
21. Pan, Y.C.; Phoong, S.M.; Lin, Y.P. An improved ESPRIT-based blind CFO estimation algorithm in OFDM systems. In Proceedings of the 2014 48th Asilomar Conference on Signals, Systems and Computers, Pacific Grove, CA, USA, 2–5 November 2014.
22. Oh, J.H.; Kim, J.G.; Lim, J.T. Blind carrier frequency offset estimation for OFDM systems with constant modulus constellations. *IEEE Commun. Lett.* **2011**, *15*, 971–973. [CrossRef]
23. Lmai, S.; Bourre, A.; Laot, C.; Houcke, S. An efficient blind estimation of carrier frequency offset in OFDM systems. *IEEE Trans. Veh. Technol.* **2013**, *63*, 1945–1950. [CrossRef]
24. Jayaprakash, A.; Reddy, G.R. Covariance-fitting-based blind carrier frequency offset estimation method for OFDM systems. *IEEE Trans. Veh. Technol.* **2016**, *65*, 10101–10105. [CrossRef]
25. Amar, A.; Avrashi, G.; Stojanovic, M. Low complexity residual doppler shift estimation for underwater acoustic multicarrier communication. *IEEE Trans. Signal Process.* **2016**, *65*, 2063–2076. [CrossRef]
26. Li, X.; Zhou, R.; Chakravarthy, V.; Hong, S.; Wu, Z. Total intercarrier interference cancellation for OFDM mobile communication systems. In Proceedings of the 2010 7th IEEE Consumer Communications and Networking Conference, Las Vegas, NV, USA, 9–12 January 2010; pp. 1–5.
27. Li, X.; Han, Q.; Ellinger, J.; Zhang, J.; Wu, Z. General total inter-carrier interference cancellation for OFDM high speed aerial vehicle communication. In Proceedings of the 2013 IEEE International Conference on Communications (ICC), Budapest, Hungary, 9–13 June 2013; pp. 4698–4702.
28. Arora, J. *Introduction to Optimum Design*, 2nd ed.; Academic Press: Oxford, UK, 2004; pp. 289–293.
29. Abdelkareem, A.E.; Sharif, B.S.; Tsimenidis, C.C.; Neasham, J.A. Time Varying Doppler-Shift Compensation for OFDM-Based Shallow Underwater Acoustic Communication Systems. In Proceedings of the IEEE International Conference on Mobile Adhoc & Sensor Systems, Washington, DC, USA, 17–22 October 2011.
30. Mason, S.F.; Berger, C.R.; Zhou, S.; Willett, P. Detection, synchronization, and Doppler scale estimation with multicarrier waveforms in underwater acoustic communication. *IEEE J. Sel. Areas Commun.* **2008**, *26*, 1638–1649. [CrossRef]
31. Parrish, N.; Roy, S.; Arabshahi, P. Symbol by symbol Doppler rate estimation for highly mobile underwater OFDM. In Proceedings of the Proceedings of the Fourth ACM International Workshop on UnderWater Networks, Berkeley, CA, USA, 3 November 2009; pp. 1–8.
32. Ceballos Carrascosa, P.; Stojanovic, M. Adaptive Channel Estimation and Data Detection for Underwater Acoustic MIMO–OFDM Systems. *IEEE J. Ocean. Eng.* **2010**, *35*, 635–646. [CrossRef]
33. Abdelkareem, A.E.; Sharif, B.S.; Tsimenidis, C.C. Adaptive time varying doppler shift compensation algorithm for OFDM-based underwater acoustic communication systems. *Ad Hoc Netw.* **2016**, *45*, 104–119. [CrossRef]
34. Tao, F.; Laili, Y.; Zhang, L. Brief history and overview of intelligent optimization algorithms. In *Configurable Intelligent Optimization Algorithm*; Springer: Berlin/Heidelberg, Germany, 2015; pp. 3–33.
35. Zhang, J.; Chen, S.; Mu, X.; Hanzo, L. Turbo multi-user detection for OFDM/SDMA systems relying on differential evolution aided iterative channel estimation. *IEEE Trans. Commun.* **2012**, *60*, 1621–1633. [CrossRef]
36. Tan, T.H.; Chang, C.C.; Jean, F.R.; Chiang, J.Y.; Lu, Y.C. Joint channel estimation and multi-user detection for OFDMA systems using a genetic algorithm with simulated annealing-based mutation. In Proceedings of the 2013 IEEE International Conference on Systems, Man, and Cybernetics, Manchester, UK, 13–16 October 2013; pp. 162–167.
37. Zhang, J.; Chen, S.; Mu, X.; Hanzo, L. Evolutionary-algorithm-assisted joint channel estimation and turbo multiuser detection/decoding for OFDM/SDMA. *IEEE Trans. Veh. Technol.* **2013**, *63*, 1204–1222. [CrossRef]

38. Li, J.; Li, L.; Yu, F.; Ju, Y.; Ren, J. Application of simulated annealing particle swarm optimization in underwater acoustic positioning optimization. In Proceedings of the OCEANS 2019-Marseille, Marseille, France, 17–20 June 2019; pp. 1–4.

39. Song, J.; Wang, Z.; Niu, Y.; Dong, H. Genetic-algorithm-assisted sliding-mode control for networked state-saturated systems over hidden Markov fading channels. *IEEE Trans. Cybern.* **2020**, *51*, 3664–3675. [CrossRef]

40. Das, S.; Mullick, S.S.; Suganthan, P.N. Recent advances in differential evolution–an updated survey. *Swarm Evol. Comput.* **2016**, *27*, 1–30. [CrossRef]

41. Tanabe, R.; Fukunaga, A. Reevaluating exponential crossover in differential evolution. In Proceedings of the International Conference on Parallel Problem Solving from Nature, Ljubljana, Slovenia, 13–17 September 2014; Springer: Berlin/Heidelberg, Germany, 2014, pp. 201–210.

42. Tanabe, R.; Fukunaga, A.S. Improving the search performance of SHADE using linear population size reduction. In Proceedings of the Evolutionary Computation, Beijing, China, 6–11 July 2014.